Journal of Science and Transport Technology
Journal homepage: https://jstt.vn/index.php/en

Sustainable Use of Coal Combustion Bottom Ash as A Fine Aggregate in Normal-Strength Concrete Production

Van-Dung Nguyen[1], Si-Huy Ngo[1], Lanh Si Ho[2], Trong-Phuoc Huynh[3,*]
[1]Faculty of Engineering, Technology, and Communication, Hong Duc University, No. 565, Quang Trung Street, Hac Thanh Ward, Thanh Hoa 40000, Vietnam
[2]Resilience & Innovative Materials for Smart Infrastructures (RIMAS), University of Transport Technology, 54 Trieu Khuc Street, Thanh Liet Ward, Hanoi 11407, Vietnam
[3]Faculty of Civil Engineering, College of Engineering, Can Tho University, Campus II, 3/2 Street, Ninh Kieu Ward, Can Tho City 94000, Vietnam

Article info
Type of article:
Original research paper

DOI:
https://doi.org/10.58845/jstt.utt.2025.en.5.4.177-197

***Corresponding author:**
Email address:
htphuoc@ctu.edu.vn

Received: 29/04/2025
Received in Revised Form: 16/11/2025
Accepted: 04/12/2025

Abstract: The construction industry's heavy reliance on natural sand and cement contributes significantly to environmental degradation, driving the need for more sustainable materials. One potential solution is the use of coal combustion bottom ash (BA), a waste by-product from coal-fired power plants, as a replacement for fine aggregates in concrete. This study investigates the use of bottom ash (BA) as a partial replacement for natural sand (0–100%) in normal-strength concrete through a comprehensive experimental program. Concrete mixtures incorporating different BA replacement levels were evaluated, focusing on the combined effects on workability, water absorption, porosity, and ultrasonic pulse velocity. Results revealed that while increasing the w/b ratio improved workability, it reduced compressive strength, with the control mixture WB36 (w/b = 0.36) achieving 30.87 MPa at 28 days. Notably, BA30 (30% BA) demonstrated a 4.5% increase in strength, while BA100 (100% BA) caused a significant 43.5% decline. Higher BA content also led to increased water absorption and porosity, with BA100 exhibiting a 122.75% increase in water absorption. Additionally, the study provides a quantitative evaluation of the environmental benefits, showing that BA30 reduces CO_2 emissions by 2.34%, while BA100 achieves a 10.55% reduction. This research demonstrates that, by carefully balancing BA content, concrete can achieve significant sustainability gains, offering a novel approach to waste valorization in construction. The findings identify BA30 as an optimal mix, offering a balanced trade-off between engineering performance and environmental impact, supporting its potential application in sustainable concrete production.
Keywords: Coal combustion bottom ash; fine aggregate; normal-strength concrete; cost analysis; environmental impacts.

1. Introduction

The construction industry plays a pivotal role in shaping modern infrastructure, urban development, and economic growth. However, it is also one of the most resource-intensive and environmentally impactful sectors worldwide.

Concrete, the most widely used construction material, consumes enormous quantities of cement, sand, gravel, and water. The production of cement alone contributes approximately 7–8% of global carbon dioxide (CO_2) emissions, while natural sand extraction has led to severe ecological disturbances, including habitat destruction, riverbank erosion, and groundwater depletion [1]. These challenges have driven a global push toward more sustainable construction practices, particularly through the substitution of virgin raw materials with industrial by-products and recycled waste streams.

Among the numerous waste materials generated by various industrial activities, coal combustion bottom ash (BA) is a significant yet underutilized by-product from thermal power plants. Typically constituting 10–20% of the total ash output from coal-fired plants, BA is a coarse, granular material that accumulates at the base of the furnace [2]. Unlike fly ash (FA), which has been extensively researched and widely accepted as a pozzolanic additive or supplementary cementitious material, BA often ends up in landfills or ash ponds, contributing to soil and water contamination and occupying valuable land [3]. The recycling of BA in construction materials offers a dual benefit [4]: mitigating the environmental impact of coal combustion residue and reducing the demand for natural sand in concrete production.

The growing emphasis on sustainable construction has led to increased interest in reusing industrial by-products such as coal combustion BA in concrete applications. BA exhibits promising characteristics, such as granular texture and potential pozzolanic activity, that make it suitable for replacing traditional concrete components like cement or fine aggregates [5]. An earlier study by Kurama and Kaya [2] demonstrated that thermally and mechanically treated BA could enhance the mechanical performance of concrete when partially replacing cement. More recent studies have shifted attention to its role as a sand substitute. Ashraf et al. [6] evaluated various replacement levels and found that 25% BA content improved the CS of concrete at 90 days, though higher proportions negatively impacted durability due to increased porosity and water absorption. Kiruthiga et al. [7] observed that pulverized BA, used as a cement replacement in concrete, enhanced strength and densified the concrete matrix due to prolonged pozzolanic reactions, while also contributing to lower emissions and reduced construction costs. In parallel, environmental assessments of BA generation have shown positive developments. Li et al. [8] studied the co-combustion of coal gangue and sludge conditioned with $FeCl_3$ and rice husk, revealing improvements in pollutant reduction and heavy metal stabilization in the resulting ash. Similarly, Zhao et al. [9] highlighted the ability of sludge ash minerals to suppress sulfur dioxide emissions and immobilize toxic metals, making the BA more suitable for reuse. The durability potential of ash-based concrete has also been examined in specialized applications; for example, Arenas et al. [10] demonstrated that incorporating both FA and BA in concrete blocks significantly improved fire resistance without sacrificing mechanical or environmental performance. Taken together, these findings suggest that coal BA, when incorporated at moderate levels (25–30%), can enhance concrete strength, reduce environmental impact, and support material circularity. However, excessive substitution levels may compromise durability, reinforcing the importance of careful mix design and material processing.

Despite these potentially advantageous properties, the utilization of BA as a fine aggregate remains limited, with existing research often constrained to partial replacements at low substitution levels (i.e., 10–30%), and frequently focused on high-performance or specialized concretes such as self-compacting or high-strength mixes. In contrast, normal-strength concrete (NSC), typically characterized by compressive strengths in the range of 20–40 MPa, remains the most prevalent concrete type used globally, especially in residential, low-rise, and general infrastructure applications [5]. However, limited studies have

systematically evaluated the use of BA as a full-range fine aggregate replacement (0–100%) in NSC. Furthermore, there is a lack of systematic assessments that integrate not only mechanical and durability properties but also sustainability metrics such as embodied CO_2 emissions, energy consumption, and economic costs.

To address these gaps, this study investigates the sustainable utilization of coal combustion BA as a fine aggregate in NSC. Concrete mixes were prepared with varying BA replacement levels (0%, 30%, 50%, 70%, and 100%) and various w/b ratios (0.36, 0.39, 0.42) to evaluate a wide design matrix. Key fresh properties, such as slump and unit weight (UW), were measured alongside hardened performance indicators, including compressive strength (CS), water absorption (WA), porosity, and ultrasonic pulse velocity (UPV). Additionally, this study quantifies the relationship between porosity and performance indicators, providing regression-based insights into the microstructural implications of BA use. Importantly, the present study also conducts a life-cycle-informed sustainability assessment, measuring CO_2-equivalent emissions (CO_2-eq), energy consumption (EC), and material costs per cubic meter of concrete. These parameters are further normalized by 28-day CS to provide a performance-adjusted view of environmental and economic efficiency, a critical perspective often overlooked in conventional concrete research. The findings of this study contribute to the broader goals of sustainable construction by offering a comprehensive evaluation of BA as a viable replacement for natural sand.

2. Materials and experimental methods

2.1. Materials

The binder used to prepare the concrete specimens was Nghi Son cement type PCB40, which has a density of 3.15 g/cm^3. The coarse aggregate used was crushed stone, with a maximum size of 12.5 mm and a density of 2.70 g/cm^3. To enhance the workability of the BA concrete mix, a type-G superplasticizer (density of 1.10 g/cm^3) was incorporated to mitigate the effects of BA on the mix's flowability.

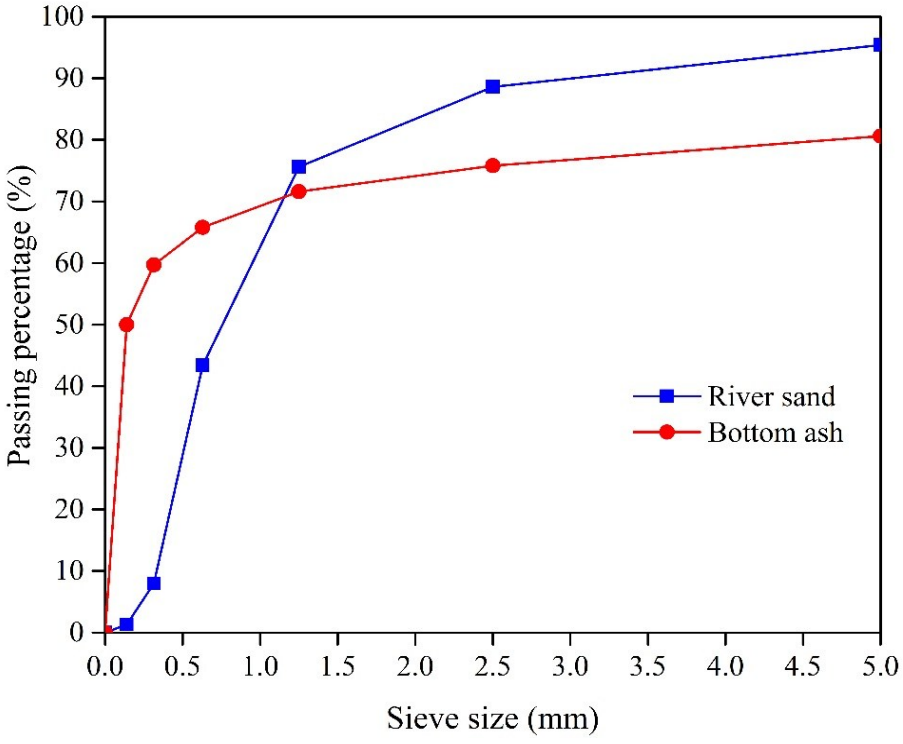

Fig. 1. Gradation curves of natural river sand and BA

In this study, BA was sourced from the Nghi Son coal thermal power plant in Thanh Hoa province, Vietnam, and natural fine aggregate was collected from the Ma River. The gradation curves and physical properties of these aggregates are shown in Fig. 1 and Table 1, respectively. As illustrated, the river sand has a relatively uniform distribution, with a significant percentage of particles passing through a 1.25 mm sieve. The curve for river sand demonstrates a gradual increase in the passing percentage as the sieve size decreases, indicating a well-graded material with a typical distribution of fine particles. On the other hand, the BA curve shows a steeper slope compared to river sand, with a higher proportion of fine particles passing through smaller sieves (less than 1.25 mm). This indicates that BA has a much finer particle size distribution, with a larger portion of particles falling into the fine aggregate category. As a result, BA tends to have a greater surface area, contributing to its higher WA and lower density than natural river sand. This difference in particle size distribution affects the performance of the two materials when used in concrete mixes, with BA's finer particles potentially influencing the workability and strength of the resulting concrete, especially at higher replacement levels.

Table 1 presents the characteristics of natural river sand and BA. The density of river sand is 2.62 g/cm^3, which is notably higher than that of BA, which has a density of 1.99 g/cm^3. This indicates that BA is less dense compared to natural river sand, making it more lightweight. In terms of unit weight, river sand has a value of 1.50 g/cm³, while BA has a lower value of 1.08 g/cm³, further supporting the notion that BA is a lighter material. The WA of BA is significantly higher, at 23.15%, compared to the 1.08% of river sand. This high WA of BA suggests that its particles are much more porous, which can influence the workability and hydration properties of concrete mixtures containing BA. Lastly, the fineness modulus of river sand is 2.83, which is higher than that of BA at 1.97. This indicates that river sand has a coarser particle gradation, while BA has finer particles on average. These differences in material properties, such as density, WA, and particle size distribution, significantly affect the performance of concrete mixtures, particularly in terms of strength, durability, and workability.

Table 1. Characteristics of natural river sand and BA

Materials	Density (g/cm^3)	Unit weight (g/cm^3)	WA (%)	Fineness modulus
River sand	2.62	1.50	1.08	2.83
BA	1.99	1.08	23.15	1.97

Fig. 2a presents the SEM image of BA particles at a magnification of 200X. To provide a broader microstructural reference for interpreting the role of BA in concrete performance, SEM images of cement particles (Fig. 2b) were also included in this study. The cement particles exhibit angular and irregular morphologies with relatively dense surfaces, contrasting with the highly porous and heterogeneous texture observed in BA particles. This comparison highlights the fundamental differences in surface characteristics and internal structure between BA and conventional cementitious materials, which directly influence water demand, pore development, and strength evolution in BA-containing concretes. The irregular shape and porous nature of BA particles, as seen in Fig. 2a, indicate that BA may have a higher surface area compared to conventional fine aggregates, influencing both workability and water absorption characteristics of the concrete mixes.

It should be noted that SEM images of natural river sand were not obtained during the experimental program. However, the morphology of river sand particles has been extensively reported in existing literature and is typically characterized by relatively smooth surfaces and lower porosity compared to BA. The inclusion of the cement's SEM image, therefore, provides an adequate morphological reference to contextualize the observed performance trends.

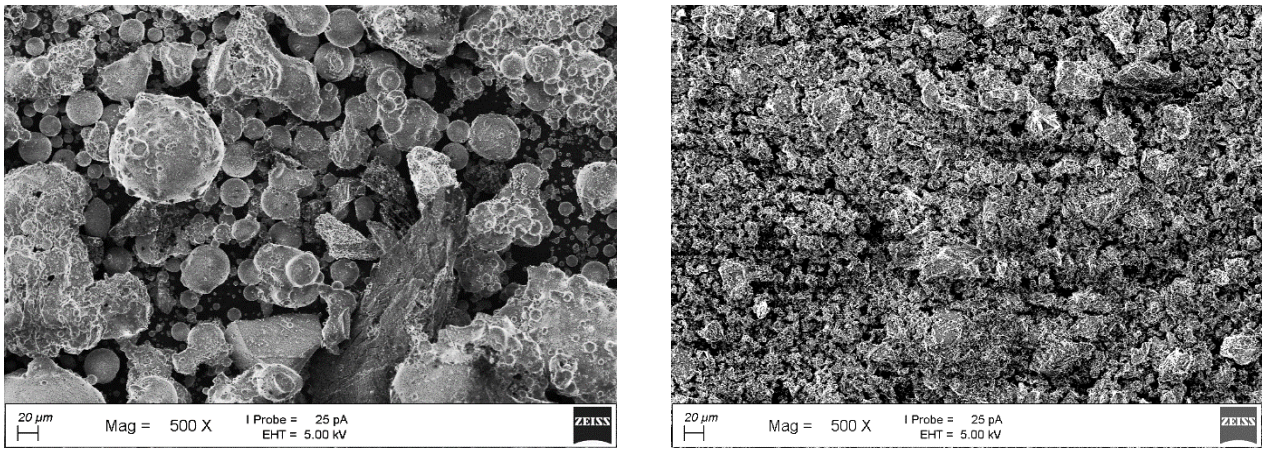

(a) BA (b) Cement

Fig. 2. SEM image of BA and cement particles.

2.2. Concrete mixture proportions

The mixture proportions of the NSC used in this study are presented in Table 2, which details the w/b ratios, BA content, and the specific quantities of all concrete ingredients for each mixture. The control mixtures (WB36, WB39, and WB42) were without BA, with varying w/b ratios of 0.36, 0.39, and 0.42, respectively. The BA-containing mixes (BA30, BA50, BA70, and BA100) incorporate BA as a partial replacement for fine aggregate (30–100% by volume) and a fixed w/b ratio of 0.36. The proportions of cement, sand, aggregate (CA), water, and superplasticizer (SP) are also provided for each mix, reflecting the adjustments made to accommodate the increasing BA content.

Given the high WA of BA (Table 1), both river sand and BA were conditioned to a saturated surface dry (SSD) state prior to mixing. The fine aggregates were pre-soaked and surface-dried to SSD to prevent uncontrolled water uptake during mixing. The mixing water shown in Table 2 represents the effective free water used to achieve the target w/b ratio, while the pre-wetting water associated with SSD aggregates was not counted toward the w/b calculation.

Table 2. Mixture proportions of concrete

Mixtures	w/b	BA content (%)	Concrete ingredient proportions (kg/m^3)					
			Cement	Sand	BA	CA	Water	SP
WB36	0.36	0	513	955	0	770	185	0.0
WB39	0.39	0	473	988	0	770	185	0.0
WB42	0.42	0	440	1017	0	770	185	0.0
BA30	0.36	30	496	647	277	745	174	5.0
BA50		50	485	452	452	729	170	4.9
BA70		70	475	265	619	713	166	4.7
BA100		100	460	0	857	691	161	4.6

2.3. Test methods

The test methods used for evaluating both the fresh and hardened properties of concrete are summarized in Table 3. The tests, including slump, fresh unit weight (UW), compressive strength (CS), water absorption (WA), porosity, and ultrasonic pulse velocity (UPV) (Fig. 3), were conducted in triplicate (except for slump and UW) following relevant standard guidelines, ensuring consistency and accuracy across the measurements.

Table 3. Summarization of test methods.

Items	Test name	Specimen's dimension (cm)	Age (day)	Standard
Fresh properties of concrete	Slump	-	-	ASTM C143 [11]
	UW	-	-	ASTM C138 [12]
Hardened properties of concrete	CS	10 × 10 × 10	3, 7, 14, 28	TCVN 3118:2022 [13]
	WA, Porosity	10 × 10 × 10	28	ASTM C642 [14]
	UPV	Ø10 × 20	3, 7, 14, 28	ASTM C597 [15]

(a) Slump (b) Fresh UW (c) WA

(d) CS (e) Porosity (f) UPV

Fig. 3. Test methods used to determine the concrete's properties

3. Results and discussion

3.1. Fresh concrete properties

The properties of fresh concrete mixtures (i.e., slump and UW) are crucial indicators, including the workability and density of the mix, which directly influence the ease of handling and durability of the hardened material. Based on the results from Table 4, significant trends were observed regarding the slump and UW of concrete as the w/b ratio and BA content varied.

Regarding the slump, which is an indicator of the workability of the concrete mix, the control mix (WB36, 0% BA) exhibited a slump of 65 mm, indicating moderate workability. As the w/b ratio

increased, the slump increased accordingly. The WB39 mix (w/b = 0.39) showed a 7.7% increase in slump (to 70 mm), and the WB42 mix (w/b = 0.42) exhibited an increase of 23.1% in slump (to 80 mm), suggesting that the higher water content in these mixes enhanced the workability of the mix, allowing for easier flow and handling. This is consistent with the fundamental understanding that higher water content increases the slump, making the mix more fluid. When BA was incorporated into the mix, the slump values showed a progressive decrease; this result is consistent with the results found in the previous studies [16, 17]. For example, the BA30 mix (30% BA) exhibited a 15.4% decrease in slump (to 55 mm), likely due to the higher water absorption and angular, porous texture of BA compared to natural sand. As the BA content increased, the workability further decreased. The BA100 mix (100% BA) showed a 69.2% decrease in slump (to 20 mm), indicating poor workability, which could complicate the handling and placement of the concrete.

Table 4. Fresh properties of concrete mixtures.

Mixtures	w/b	BA content (%)	Fresh properties		
			Slump (mm)	UW (kg/m^3)	UW change (%)
WB36	0.36	0	65	2326	0
WB39	0.39	0	70	2299	-1.16
WB42	0.42	0	80	2306	-0.86
BA30	0.36	30	55	2233	-4.00
BA50		50	50	2174	-6.53
BA70		70	35	2092	-10.06
BA100		100	20	2018	-13.24

Regarding UW, the WB36 mix showed a UW of 2326 kg/m³, which is typical for conventional concrete mixes. As the w/b ratio increased, the UW decreased slightly. The WB39 mix (w/b = 0.39) had a 1.16% reduction in UW (to 2299 kg/m³), and the WB42 mix (w/b = 0.42) showed a 0.86% reduction (to 2306 kg/m³). These decreases reflect the dilution of the cement content with excess water, which reduces the overall density of the concrete, though the changes were relatively minor. The incorporation of BA resulted in a more noticeable reduction in UW, which is attributed to the porous structure and low density of BA, as indicated in the previous studies [17–19]. For instance, the BA30 mix showed a 4.00% decrease in UW (to 2233 kg/m³), which can be attributed to the lower density of BA compared to natural sand. The trend continued as the BA content increased: BA50 showed a 6.53% reduction (to 2174 kg/m³), BA70 had a 10.06% reduction (to 2092 kg/m³), and BA100 exhibited a 13.24% reduction (to 2018 kg/m³). These findings indicate that higher BA contents result in lower-density concrete, which is mainly due to the higher porosity and lower particle density of BA compared to traditional fine aggregates (i.e., natural river sand).

3.2. Compressive strength

The CS of the NSC mixes (Fig. 4) revealed significant differences based on the w/b ratio. The WB36 mix with w/b of 0.36 demonstrated the highest CS at all curing times, with a final strength of 30.87 MPa at 28 days. In comparison, WB39 (w/b = 0.39) showed a 9.6% reduction in strength, reaching 27.7 MPa at 28 days, and WB42 (w/b = 0.42) exhibited a 16.2% reduction, with a final strength of 25.86 MPa at 28 days. This data demonstrates a clear trend where increasing the w/b ratio reduces the CS of the concrete.

At 3 days, WB36 achieved 17.35 MPa, whereas WB39 and WB42 showed strengths of 14.83 MPa and 14.66 MPa, respectively. The strength reduction at early stages was also

significant, with WB39 showing a 14.4% lower strength and WB42 exhibiting a 15.4% lower strength than WB36. At 7 days, the WB36 mix continued to outperform the others, reaching 25.43 MPa. WB39 had a 15.0% reduction (21.61 MPa), and WB42 showed a 17.0% reduction (21.05 MPa). By this point, the effect of the w/b ratio on strength was more pronounced; a higher w/b ratio led to lower early-age strength. By 28 days, the trend continued, with WB36 showing the highest strength (30.87 MPa), while WB39 and WB42 exhibited strength reductions of 10.1% and 16.2%, respectively. Based on these results, all investigated mixtures can be classified as NSC, as the measured 28-day CS ranges from 17.47 to 32.25 MPa, which falls within the commonly accepted strength range for NSC (20–40 MPa) [5], considering practical variability in mix design and material selection. This confirms that the proposed BA–based mixtures are directly applicable to conventional concrete construction rather than specialized high-strength systems. The results also underscore the critical role of the w/b ratio in determining both early-age and long-term CS development.

The strength reduction with increasing w/b ratios is consistent with previous studies that highlight the trade-off between higher workability and lower strength [20]. WB36, with a w/b ratio of 0.36, benefitted from lower water content, resulting in a denser, more compact structure with higher early and long-term strength.

The observed reduction in CS with increasing w/b ratio is due to the dilution of cement particles by excess water, which creates a less dense microstructure. Higher water content leads to the formation of capillary pores, increasing porosity and reducing internal cohesion, thus weakening the bond structure. In contrast, a lower w/b ratio, like in WB36, results in a denser matrix with fewer voids, enhancing both strength and durability. These results highlight the crucial role of the w/b ratio in mix design, where lower w/b ratios improve CS, as seen in WB36. Conversely, higher w/b ratios, such as in WB39 and WB42, create a more porous structure, leading to decreased strength. This aligns with the well-established relationship between the w/b ratio and CS in concrete [20], emphasizing the balance needed between workability and strength in the mix design.

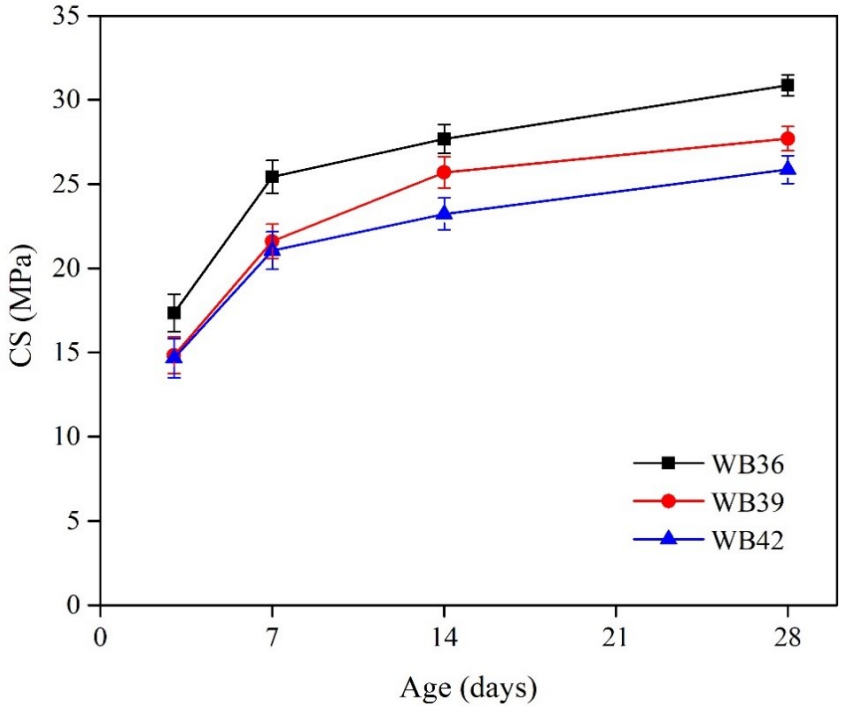

Fig. 4. CS development of NSC with different w/b ratios

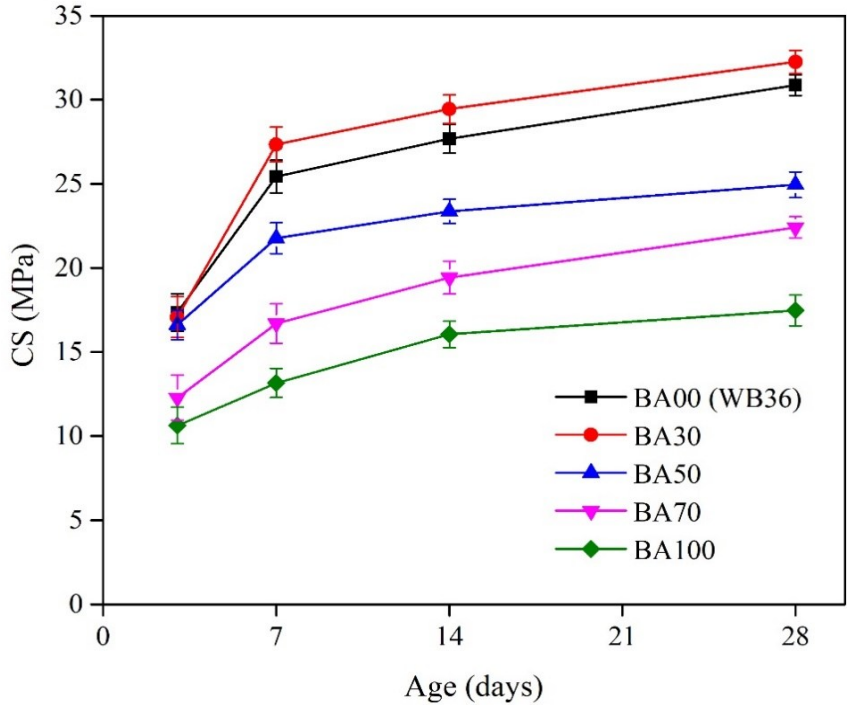

Fig. 5. CS development of concretes with various BA contents

The CS results, shown in Fig. 5, illustrate the effect of BA content on NSC's strength at different curing ages. At 3 days, the WB36 (BA00) mix exhibited a strength of 17.35 MPa, which was higher than all BA-containing mixes. The BA30 mix (30% BA) showed a minor decrease in CS to 17.07 MPa, a reduction of only 1.6% compared to the control, indicating that the addition of BA at this level does not significantly hinder early strength development. However, as the BA content increased, the CS at 3 days decreased more sharply, with BA50 at 16.62 MPa (a 4.2% reduction), BA70 at 12.28 MPa (a 29.3% reduction), and BA100 at 10.63 MPa (a 38.9% reduction) relative to the control mix. After 7 days of curing, the 30% BA mix (BA30) performed relatively well, showing 27.34 MPa, a 7.5% improvement over the control mix (25.43 MPa). This suggests that the reactive component in BA was contributing to strength development through pozzolanic reactions. However, as the BA content increased, the CS continued to decline. The BA50 mix showed 21.77 MPa (a 14.5% reduction), while BA70 and BA100 exhibited 16.69 MPa (a 34.5% reduction) and 13.16 MPa (a 48.2% reduction), respectively. These trends indicate that while 30% BA can enhance early strength, higher BA contents delay the pozzolanic reaction, limiting early strength development.

At 14 days, the BA30 mix continued to show promising results, reaching 29.45 MPa, a 6.4% improvement compared to BA00 (WB36) at 27.68 MPa, confirming that 30% BA is beneficial for both early and medium-term strength development. On the other hand, BA50 exhibited 23.36 MPa (a 15.7% reduction), BA70 had 19.42 MPa (a 29.7% reduction), and BA100 had 16.05 MPa (a 41.8% reduction). These reductions reflect the increasing porosity and slower hydration of the cement matrix as more BA is incorporated into the mix. At the critical 28-day curing period, the CS of the BA30 mix reached 32.25 MPa, showing a 4.5% improvement over the control mix (30.87 MPa), which indicates that the pozzolanic effect of active components in BA is still contributing positively to strength development at this stage. However, the mixes with higher BA content showed notable reductions in strength: BA50 exhibited 24.95 MPa (a 19.2% reduction), BA70 showed 22.41 MPa (a 27.6% reduction), and BA100 achieved 17.47 MPa (a 43.5% reduction) at 28 days. The significant

reduction in CS at higher BA levels is primarily due to the increased porosity caused by the slower pozzolanic reaction of BA compared to cement, which results in a less dense and less cohesive microstructure. The reduction of CS with the increase of BA content obtained in this study conformed to the results found in the previous studies [17, 21–23].

In summary, the results demonstrate that 30% BA replacement (BA30) provides the best balance of strength and sustainability, with a 4.5% improvement in CS at 28 days compared to the control mix. However, as BA content increases beyond 50%, the CS decreases significantly, particularly after 28 days. These reductions are mainly due to the slower hydration of BA and the resulting increase in porosity, which weakens the concrete. The findings highlight the importance of optimizing BA content to maintain adequate strength while benefiting from the environmental advantages of using industrial by-products like BA.

3.3. Water absorption and porosity

The incorporation of BA significantly affected the WA and porosity of hardened concrete (Table 5). For the control mixes with no BA (i.e., WB36, WB39, and WB42), the WA and porosity increased as the w/b ratio increased. WB36 (w/b = 0.36) exhibited the lowest WA of 2.33% and porosity of 3.65%. As the w/b ratio increased, WB39 (w/b = 0.39) showed a 6.01% increase in WA (2.47%) and a 10.96% increase in porosity (4.05%), while WB42 (w/b = 0.42) showed a 24.03% increase in WA (2.89%) and a 12.60% increase in porosity (4.11%). This trend confirms the general understanding that higher w/b ratios lead to more porous structures with higher water absorption, which is typically associated with weaker concrete properties.

Table 5. Water absorption and porosity of hardened concrete

Mixtures	w/b	BA content (%)	WA (%)	WA change (%)	Porosity (%)	Porosity change (%)
WB36	0.36	0	2.33	0	3.65	0.00
WB39	0.39	0	2.47	+6.01	4.05	+10.96
WB42	0.42	0	2.89	+24.03	4.11	+12.60
BA30	0.36	30	2.18	-6.44	3.05	-16.44
BA50		50	3.59	+54.08	4.31	+18.08
BA70		70	4.05	+73.82	5.44	+49.04
BA100		100	5.19	+122.75	6.81	+86.58

When BA was introduced into the mix, the effect on WA and porosity was more pronounced with increasing BA content. The BA30 mix (30% BA) showed a 6.44% decrease in WA (2.18%) and a 16.44% reduction in porosity (3.05%), indicating that the use of BA at this level resulted in denser concrete with less water absorption. This improvement may be attributed to a packing/filler effect at moderate BA replacement, where finer BA particles help fill voids within the fine aggregate skeleton and improve particle packing, thereby reducing the measured open porosity and water absorption in the BA30 mixture. As the BA content further increased to 50%, 70%, and 100%, both WA and porosity increased significantly. The BA50 mix (50% BA) showed a 54.08% increase in WA (3.59%) and an 18.08% increase in porosity (4.31%), reflecting the reduction in cement content and the introduction of more porous material (BA) into the mix. For BA70 (70% BA), WA increased to 4.05%, a 73.82% rise compared to the control, and porosity increased by 49.04% to 5.44%. Finally, the BA100 mix (100% BA) exhibited the highest increases in both WA (5.19%) and porosity (6.81%), with 122.75% and 86.58% increases, respectively, compared to WB36. This shows that

at high BA contents, the concrete becomes significantly more porous, which results in higher WA and lower overall strength and durability. From a durability perspective, the significantly higher intrinsic water absorption of BA (23.15%) compared to natural river sand (1.08%) may raise concerns regarding long-term performance, particularly under freeze–thaw cycles and in aggressive environments. Increased concrete porosity and water absorption can facilitate moisture ingress, thereby increasing the risk of freeze–thaw damage, chloride penetration, and sulfate attack [17, 24–26]. However, it should be noted that these durability risks are strongly dependent on the resulting concrete microstructure rather than the raw aggregate properties alone. In this study, the BA30 mixture exhibited reduced water absorption and porosity compared to the control mix, suggesting a denser matrix that may mitigate long-term durability concerns, whereas higher BA replacement levels (≥50%) may require additional mix optimization or durability-oriented testing. However, the BA30 mix, with 30% BA replacement, provided a balanced performance, showing a reduction in both WA and porosity, suggesting that BA at this level can enhance sustainability without sacrificing durability.

3.4. Ultrasonic pulse velocity

The UPV results, presented in Fig. 6, provide valuable insights into the internal quality and compactness of the concrete mixes. The WB36 mix (w/b = 0.36) exhibited the highest UPV at all curing stages, indicating the most compact microstructure.

At 3 days, WB36 achieved a UPV of 3938 m/s, significantly higher than both WB39 (3213 m/s) and WB42 (2923 m/s). The WB39 mix (w/b = 0.39) showed an 18.5% reduction in UPV compared to WB36, and the WB42 mix (w/b = 0.42) demonstrated a 25.8% reduction, suggesting that higher w/b ratios lead to less dense and more porous concrete.

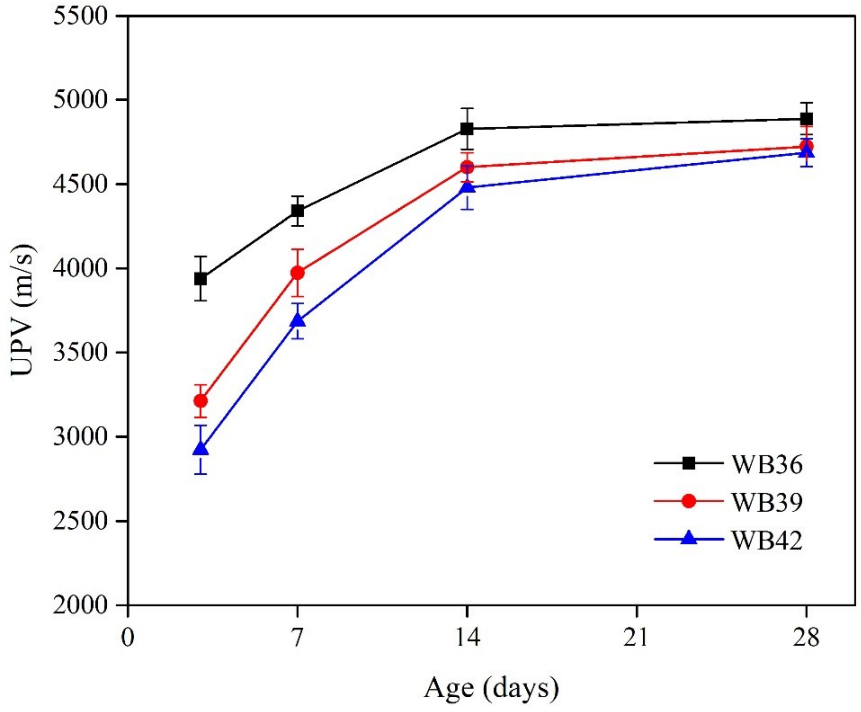

Fig. 6. UPV of concretes with different w/b ratios

The trends continued to 7 days of curing age, with WB36 showing a UPV of 4340 m/s, compared to 3973 m/s for WB39 (an 8.4% reduction) and 3686 m/s for WB42 (a 15.1% reduction). The increase in UPV with time indicates that the hydration process is progressing, and the concrete is becoming denser, particularly for the mix with the lowest w/b ratio. The increased w/b ratios in WB39

and WB42 still resulted in lower internal cohesion, as reflected in the reduced UPV values. By 14 days, WB36 had reached 4828 m/s, while WB39 and WB42 showed 4600 m/s (a 4.7% reduction) and 4479 m/s (a 7.2% reduction), respectively. The relatively slow but steady increase in UPV for the control mix indicates continued hydration and densification of the material, contributing to better internal quality. The differences in UPV between the mixes demonstrate that WB36 maintained a more uniform and cohesive structure, while WB39 and WB42 exhibited lower cohesion, as the increased water content diluted the cement and led to more porosity. At 28 days, WB36 achieved the highest UPV value of 4888 m/s, indicating a well-hydrated, dense, and well-compacted concrete matrix. In contrast, WB39 showed 4723 m/s (a 3.4% reduction), and WB42 exhibited 4686 m/s (a 4.1% reduction). These values reinforce the conclusion that the lower w/b ratio leads to a more compact and less porous structure, resulting in higher UPV, which is a key indicator of improved internal material quality and strength.

In summary, the UPV results demonstrate a strong correlation with the water-to-binder ratio, where lower w/b ratios lead to higher UPV values due to denser, less porous microstructures. The higher w/b ratios in WB39 and WB42 resulted in reduced UPV, reflecting lower material density and internal cohesion. These results are consistent with the well-established understanding that denser and more compact concrete leads to faster propagation of ultrasonic waves, which is indicative of stronger and more durable concrete.

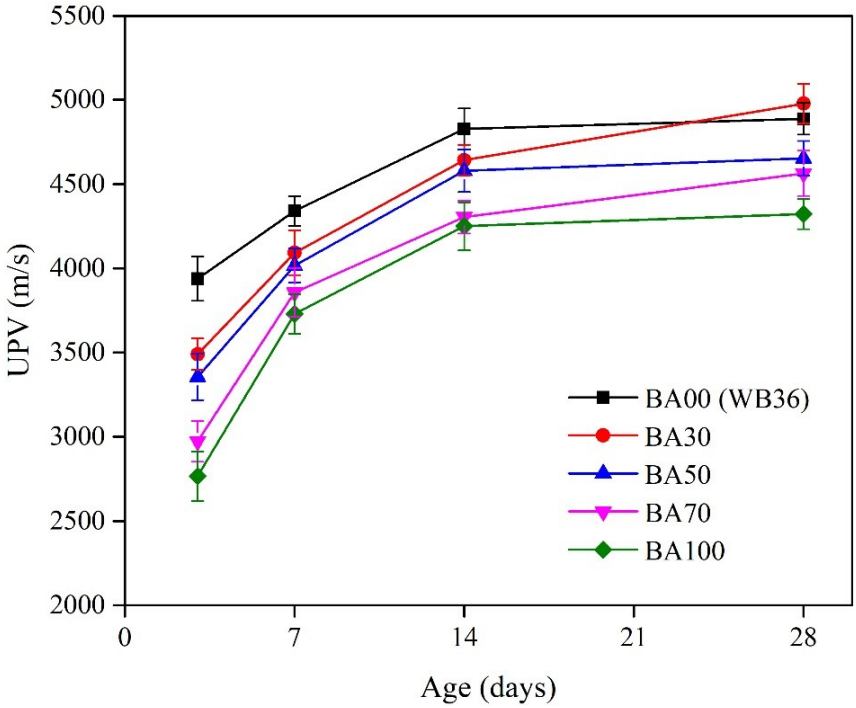

Fig. 7. UPV of concretes with various BA contents

The incorporation of BA as a fine aggregate replacement significantly influenced the UPV of the concrete mixtures (Fig. 7). At 3 days, the BA00 (WB36) control mix exhibited the highest UPV of 3938 m/s, which was higher than all BA-containing mixes. The BA30 mix (30% BA) showed an 11.4% reduction in UPV, with a value of 3490 m/s, indicating a slight decrease in material density due to the inclusion of BA. As the BA content increased further, the UPV values continued to decline: BA50 showed 3355 m/s (14.8% reduction), BA70 exhibited 2972 m/s (24.5% reduction), and BA100 showed 2766 m/s (29.7% reduction). This result agrees with the results achieved in previous research on the studies of concrete containing BA [18, 23]. These reductions suggest that increasing BA content leads to a less dense concrete structure with greater porosity, which reduces the

propagation speed of ultrasonic waves. At 7 days, the trend persisted, with the BA30 mix showing a 5.5% decrease in UPV (4092 m/s) compared to the control (4340 m/s). The BA50 mix showed a 7.5% reduction (4016 m/s), BA70 exhibited an 11.1% reduction (3856 m/s), and BA100 showed the greatest reduction of 14.0% (3729 m/s). As curing progressed, the pozzolanic reactions in the BA-containing mixes began to improve, but the reduction in UPV still reflected the higher porosity and slower hydration of BA compared to cement.

At 14 days, the BA30 mix showed 4642 m/s, a 3.9% increase from 7 days, indicating some densification over time, while BA50 showed 4579 m/s (a 3.7% reduction from BA30). The BA70 and BA100 mixes continued to show reduced UPV, with values of 4304 m/s and 4250 m/s, respectively. The lower UPV values for higher BA mixes at this stage highlight the slower pozzolanic reaction and the increasing number of voids in the matrix, leading to a less cohesive material structure. By 28 days, the BA30 mix showed the highest UPV among the BA mixes, with 4978 m/s, representing an improvement over the control mix (4888 m/s) by 1.8%. This increase suggests that, at 30% BA, the pozzolanic reactions are sufficiently active to improve internal cohesion and microstructure, enhancing the propagation of ultrasonic waves. However, the mixes with higher BA content showed a decrease in UPV: BA50 reached 4653 m/s (a 4.8% reduction from BA00), BA70 exhibited 4564 m/s (a 6.6% reduction), and BA100 showed 4322 m/s (an 11.5% reduction). These reductions further confirm that higher BA contents introduce more voids and a slower rate of cement hydration, which negatively impacts the internal quality of the concrete.

In summary, the UPV results reveal a clear inverse relationship between BA content and material density. The incorporation of 30% BA (BA30 mix) improved or maintained the UPV, suggesting a balance between sustainability and material integrity. However, higher BA contents (50% and above) significantly reduced UPV, indicating that while BA improves sustainability, its higher replacement levels lead to increased porosity and slower pozzolanic reactions, resulting in lower material density and internal cohesion. These findings underscore the trade-off between environmental benefits and mechanical performance when incorporating BA into concrete.

3.5. Correlation among concrete properties

The relationship between porosity and CS (Fig. 8) follows a negative linear trend described by the equation $y = 43.4 - 3.9x$ ($R^2 = 0.93$), where y represents the CS (MPa) and x represents the porosity (%). The negative slope indicates that each 1% increase in porosity leads to an average reduction of approximately 3.9 MPa in CS, demonstrating the high sensitivity of load-bearing capacity to pore development in BA-containing concrete.

At low porosity levels (around 3.0%), the concrete exhibited higher CS (about 30-33 MPa), as seen in mixes such as BA30 with 30% BA. In contrast, as porosity increased (to values exceeding 5.0%), such as in mixes like BA100 (100% BA), the CS dropped substantially, reaching values as low as 17-18 MPa. The negative correlation highlights the importance of controlling porosity in concrete mix design. High levels of coal combustion BA, particularly at 50% BA and above, resulted in increased porosity and a corresponding decrease in CS. This relationship underscores the challenges of using waste materials like BA in concrete, as while they offer sustainability benefits, they also introduce greater voids that reduce the material's mechanical performance.

The relationship between porosity and UPV (Fig. 9) is described by the regression equation $y = 5430.3 - 165.4x$ ($R^2 = 0.92$), indicating that UPV decreases by approximately 165 m/s for every 1% increase in porosity.

This relatively steep slope highlights the pronounced influence of pore connectivity and internal defects on ultrasonic wave propagation, confirming UPV as a sensitive indicator of microstructural degradation in BA-containing

concrete. At low porosity levels (around 3.0%), concrete exhibited higher UPV values. For example, the BA30 mix (30% BA) showed an initial UPV of nearly 5000 m/s. As the porosity increased, however, UPV values dropped significantly. For instance, at 4.0% porosity, the UPV dropped to 4700 m/s, and by 6.8% porosity, the UPV further decreased to around 4300 m/s.

The results show that the BA30 mix, which had the lowest porosity among the BA-containing mixes, maintained a relatively higher UPV compared to the higher BA mixes like BA70 and BA100, which showed significantly lower UPV values.

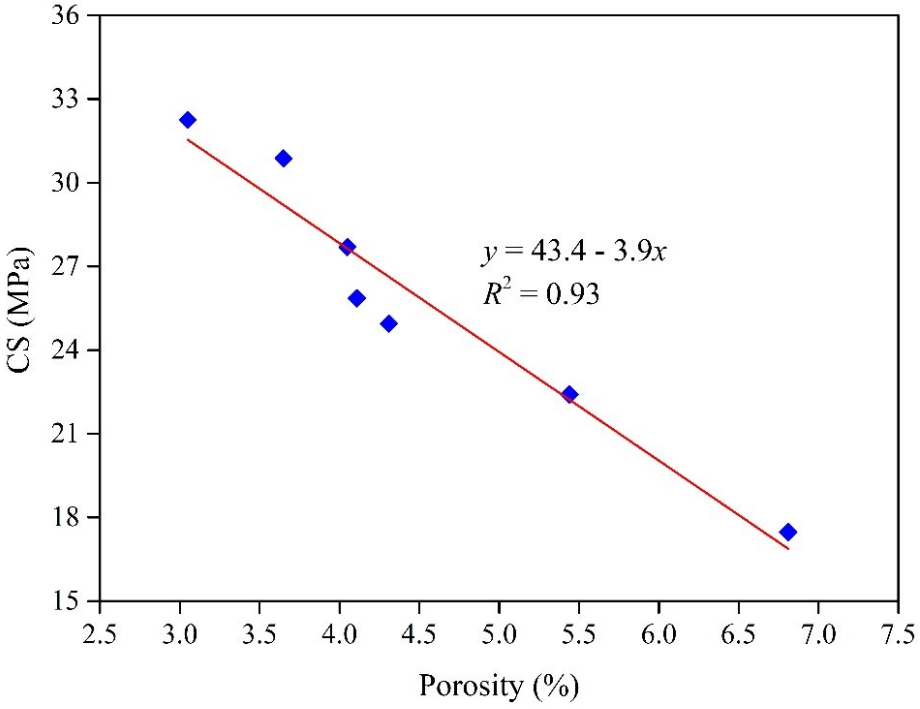

Fig. 8. Correlation between porosity and CS of concretes

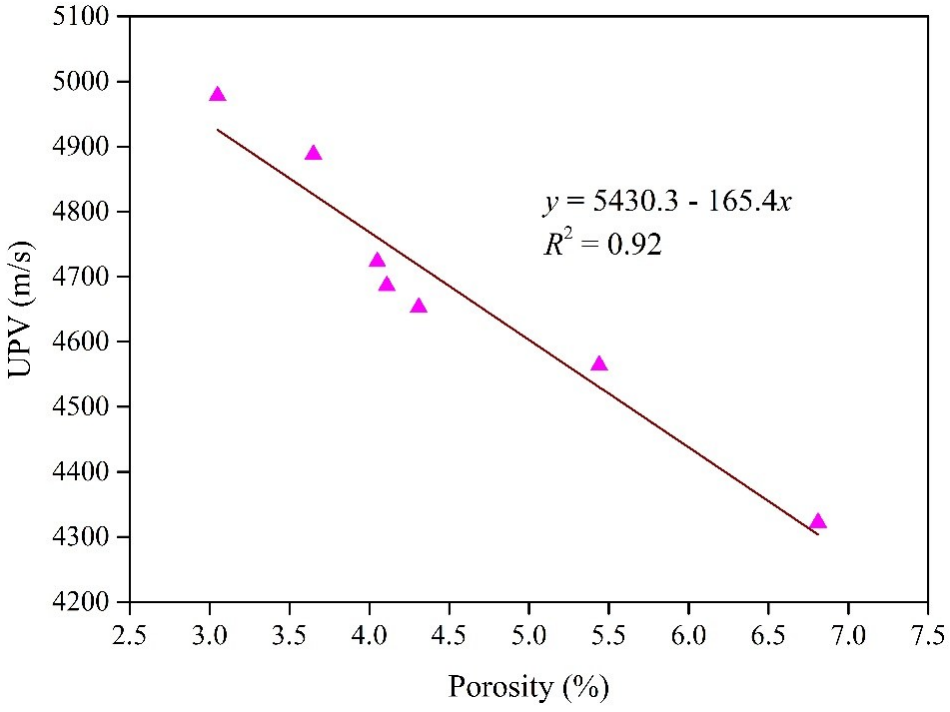

Fig. 9. Correlation between porosity and UPV of concretes

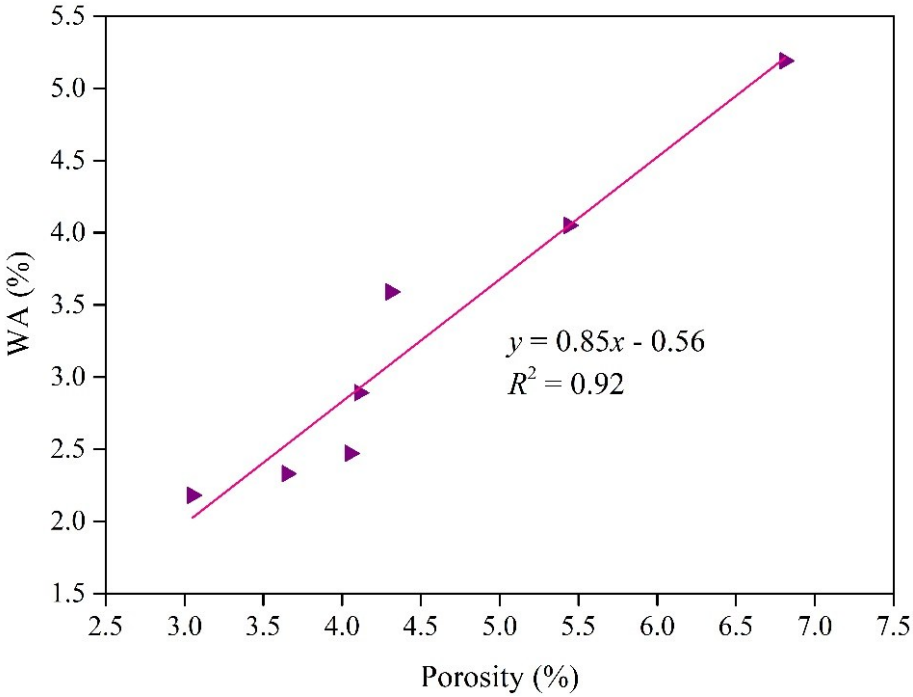

Fig. 10. Correlation between porosity and WA of concretes

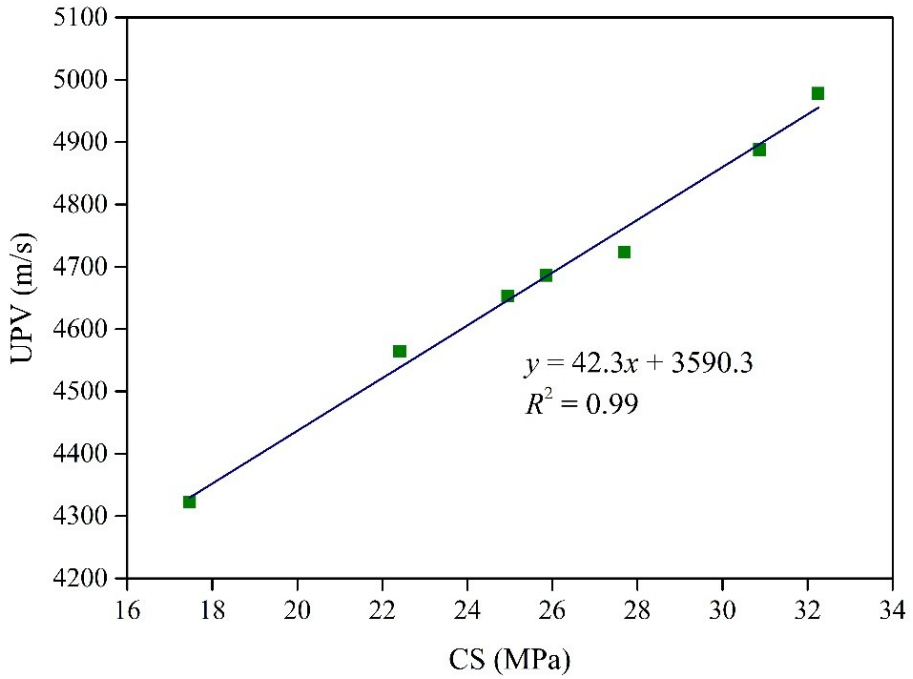

Fig. 11. Correlation between CS and UPV of concretes

The positive linear relationship between porosity and WA (Fig. 10) is expressed by $y = 0.85x - 0.56$ ($R^2 = 0.92$), indicating that each 1% increase in porosity results in an approximate 0.85% increase in WA. The magnitude of this slope quantitatively confirms that pore volume expansion directly governs moisture ingress in BA-containing concrete [27]. Concrete exhibited relatively low WA associated with low porosity, as seen in the BA30 mix (30% BA), with a WA of 2.18%. However, as porosity increased, WA rose significantly. For instance, at 4.0% porosity, the WA increased to 2.8%, and as porosity reached 6.8%, the WA rose to 5.2%, indicating a substantial increase in permeability. The data shows that higher porosity, such as in BA100, results in a higher volume of voids that allow for greater water penetration, increasing the absorption rate. The positive

correlation between WA and porosity is expected, as higher porosity typically allows for more interconnected voids that act as channels for water to pass through. As the BA content increases, the pozzolanic reaction slows down, and the resulting concrete matrix becomes more porous, increasing WA. These findings underscore the trade-off between using BA for sustainability and its effect on material durability, as higher WA can lead to higher vulnerability to freeze-thaw cycles and chemical attacks over time.

The strong positive relationship between CS and UPV (Fig. 11) is described by $y = 42.3x + 3590.3$ ($R^2 = 0.99$), indicating that relatively small changes in UPV correspond to substantial variations in CS. This reflects the close coupling between internal compactness and mechanical performance in BA-containing concrete [18, 28]. However, mixes with higher BA content, such as BA100, show much lower CS and UPV, illustrating how increased porosity and slower hydration can impair both the mechanical and acoustic properties of the material.

3.6. Analysis of cost and environmental impacts

The environmental impact and cost analysis of the concrete mixtures, presented in Table 6, provides insight into the sustainability and economic implications of incorporating coal combustion BA as a replacement for traditional fine aggregates. At the baseline, WB36 (0% BA) shows the highest values for CO_2-eq, energy consumption (EC), and material cost, with 487.6 kg/m³, 2613.6 MJ/m³, and 1281×10^3 VND/m³, respectively. As expected, increasing the w/b ratio in WB39 (w/b = 0.39) and WB42 (w/b = 0.42) leads to a decrease in all three parameters: CO_2-eq, EC, and cost. For instance, WB39 exhibits a 7.08% reduction in CO_2-eq, a 6.24% reduction in EC, and a 4.44% reduction in material cost compared to WB36. Similarly, WB42 shows a 12.91% reduction in CO_2-eq, an 11.37% reduction in EC, and an 8.07% reduction in cost compared to WB36, highlighting the environmental and economic benefits of slightly higher water content in the mix.

The incorporation of BA into the mixes showed a more nuanced effect on sustainability and cost. The BA30 mix (30% BA) resulted in a 2.34% reduction in CO_2-eq (476.2 kg/m³) compared to the control mix, as BA itself contributes some carbon emissions during its production. However, BA30 had a negligible decrease in EC of just 0.59% and a significant increase in material cost of 5.79%. The increase in cost is primarily due to the higher cost of BA compared to natural sand, despite the environmental benefits of using an industrial by-product. The higher cost of BA in comparison with natural sand can be attributed to sourcing and processing. Further increases in BA content (i.e., BA50, BA70, and BA100) generally lead to further reductions in CO_2-eq and EC, indicating that higher BA content can help reduce the overall environmental impact. For instance, BA50 shows a 4.83% reduction in CO_2-eq, a 4.10% reduction in EC, and a 0.74% increase in material cost, while BA100 leads to a 10.55% reduction in CO_2-eq, a 12.20% reduction in EC, and an 11.08% reduction in material cost. These findings indicate that using BA as a partial replacement for natural fine aggregate provides significant environmental benefits, particularly in terms of reducing CO_2 emissions and energy consumption. However, the economic impact varies depending on the BA content. The BA30 mix shows the best compromise between environmental impact and cost, with the slightest increase in cost compared to the control mix, but with notable reductions in CO_2-eq and EC. As the BA content increases beyond 30%, there is a trade-off between reduced CO_2-eq and EC versus the higher material cost, with BA100 offering the greatest environmental benefit but at the highest cost.

Fig. 12 illustrates the relative environmental impact and cost efficiency of concrete mixes when normalized by their 28-day CS. To minimize subjectivity associated with weighting-based decision models, environmental and economic

indicators were normalized by the 28-day CS, providing a performance-adjusted comparison of sustainability. This approach enables an objective ranking of mixtures without introducing externally defined weighting factors. The analysis of CO_2-eq, EC, and material cost for each m³ of concrete per 28-day CS, presented in Fig. 12 and Table 6, reveals key insights into the environmental and economic trade-offs of incorporating coal combustion BA in concrete mixes. For the control mix, BA00 (WB36), the CO_2-eq is 15.8 kg/m³·MPa, EC is 84.66 MJ/m³·MPa, and the material cost is 41.48×10³ VND/m³·MPa. This serves as the baseline for comparison of environmental impact and cost per unit of CS. As the w/b ratio increases in WB39 (w/b = 0.39) and WB42 (w/b = 0.42), all three parameters (CO_2-eq, EC, and material cost) increase, but the percentage increase is more prominent for WB42 compared to WB39. Specifically, WB39 shows a 5.8% increase in CO_2-eq (to 16.36 kg/m³·MPa), a 4.5% increase in EC (to 88.46 MJ/m³·MPa), and a 6.7% increase in material cost (to 44.18×10³ VND/m³·MPa). Meanwhile, WB42 shows a 4.2% increase in CO_2-eq (to 16.42 kg/m³·MPa), a 1.2% increase in EC (to 89.58 MJ/m³·MPa), and a 3.2% increase in cost (to 45.53×10³ VND/m³·MPa), demonstrating that a higher w/b ratio leads to slightly higher environmental impact and material costs.

Table 6. Total CO_2-eq, EC, and material cost for each m³ of concrete mixtures

Mixtures	CO_2-eq (kg/m³)	CO_2-eq change (%)	EC (MJ/m³)	EC change (%)	Cost (VND ×1000/m³)	Cost change (%)
WB36	487.6	0	2613.6	0	1281	0
WB39	453.1	-7.08	2450.5	-6.24	1224	-4.44
WB42	424.7	-12.91	2316.5	-11.37	1177	-8.07
BA30	476.2	-2.34	2598.1	-0.59	1355	+5.79
BA50	464.1	-4.83	2506.5	-4.10	1290	+0.74
BA70	452.7	-7.16	2418.4	-7.47	1225	-4.31
BA100	436.2	-10.55	2294.6	-12.20	1139	-11.08

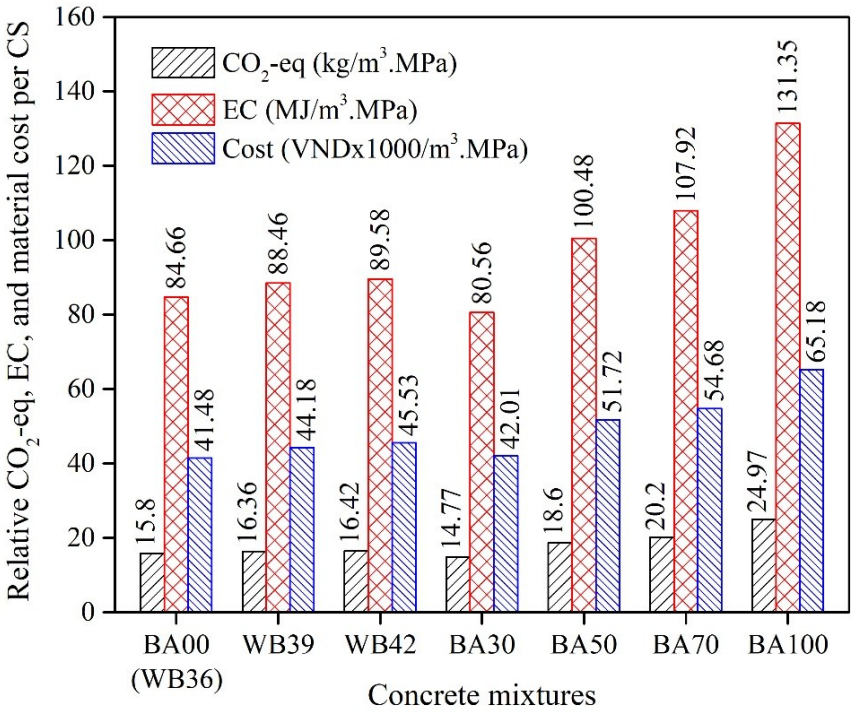

Fig. 12. Relative CO_2-eq, EC, and material cost per 28-day CS of concrete

The BA30 mix (30% BA) shows a slight environmental benefit with a 2.34% reduction in CO_2-eq (to 14.77 kg/m³·MPa) and a 0.59% reduction in EC (to 80.56 MJ/m³·MPa) compared to BA00. However, the cost increases by 1.3% (to 42.01×10^3 VND/m³·MPa), suggesting that the use of BA at 30% replacement brings some sustainability benefits but also results in a moderate increase in the cost due to BA's higher price compared to traditional fine aggregates. As the BA content increases to 50% (BA50), 70% (BA70), and 100% (BA100), the normalized CO_2-eq and EC per unit compressive strength increase, indicating that although total CO_2-eq and EC decrease, the reduced mechanical performance leads to higher environmental intensity per MPa. BA50 shows a 17.7% increase in CO_2-eq (to 18.6 kg/m³·MPa), an 18.7% increase in EC (to 100.48 MJ/m³·MPa), and a 24.7% increase in material cost (to 51.72×10^3 VND/m³·MPa) compared to BA00. For BA70, the increases are even more substantial: 20.2 kg/m³·MPa for CO_2-eq (a 28.0% increase), 107.92 MJ/m³·MPa for EC (a 27.5% increase), and 54.68×10^3 VND/m³·MPa for cost (a 31.8% increase). BA100, with 100% BA, exhibits the highest increases, with CO_2-eq reaching 24.97 kg/m³·MPa (a 58.3% increase), EC at 131.35 MJ/m³·MPa (a 55.2% increase), and cost at 65.18×10^3 VND/m³·MPa (a 57.3% increase), highlighting the trade-offs between the environmental benefits of BA and the economic costs.

In summary, the use of BA results in significant reductions in CO_2 emissions and energy consumption at lower replacement levels (such as 30% BA), with only a moderate increase in material cost. However, as BA content increases beyond 30%, the economic and environmental benefits start to diminish, and the material costs increase significantly. BA30 provides a balanced compromise between environmental impact and economic feasibility, while higher BA contents like BA100 offer substantial environmental savings but at a much higher cost. These findings emphasize the need for a careful balance between sustainability goals and cost efficiency when using industrial by-products like BA in concrete production.

4. Conclusion

This study investigates the use of BA as a partial replacement for natural fine aggregates in NSC, evaluating its effects on material performance, environmental impact, and cost efficiency. The results demonstrate the potential of BA as a sustainable alternative, with the following key findings:

• The CS test results show that the control mix (WB36) exhibited the highest CS at 30.87 MPa at 28 days. The BA30 mix (30% BA) showed a 4.5% improvement in CS (to 32.25 MPa), while BA50 (50% BA) showed a 19.2% reduction (to 24.945 MPa), BA70 (70% BA) exhibited a 27.6% reduction (to 22.41 MPa), and BA100 (100% BA) reached 17.47 MPa, a 43.5% reduction. This reduction is mainly due to increased porosity and the slower pozzolanic reaction of BA.

• Based on the WA and porosity results, the control mix (WB36) had 2.33% WA and 3.65% porosity. The BA30 mix showed a 6.44% decrease in WA (to 2.18%) and a 16.44% decrease in porosity (to 3.05%), indicating better density. However, higher BA content increased both WA and porosity: BA100 exhibited a 122.75% increase in WA (to 5.19%) and an 86.58% increase in porosity (to 6.81%), showing a significant deterioration in material integrity.

• The control mix (WB36) achieved 4888 m/s in UPV at 28 days. The BA30 mix showed a 1.8% increase (to 4978 m/s), suggesting a denser microstructure. However, as BA content increased, UPV decreased: BA50 had a 4.8% reduction (to 4653 m/s), BA70 showed a 6.6% reduction (to 4564 m/s), and BA100 exhibited an 11.5% reduction (to 4322 m/s), indicating lower internal cohesion.

• Regarding the environmental impact, the control mix (WB36) showed 487.6 kg/m³ CO_2-eq. The BA30 mix showed a 2.34% reduction in CO_2-eq (to 476.2 kg/m³), while BA50 showed a 4.83%

reduction (to 464.1 kg/m³), BA70 a 7.16% reduction (to 452.7 kg/m³), and BA100 a 10.55% reduction (to 436.2 kg/m³), indicating significant reductions in CO_2 emissions with higher BA content. Besides, the EC analysis shows that the control mix (WB36) had 2613.6 MJ/m³ EC. The BA30 mix showed a 0.59% reduction (to 2598.1 MJ/m³), while higher BA contents resulted in further reductions: BA50 showed a 4.10% reduction (to 2506.5 MJ/m³), BA70 had a 7.47% reduction (to 2418.4 MJ/m³), and BA100 exhibited a 12.20% reduction (to 2294.6 MJ/m³), indicating energy savings from BA incorporation.

• The control mix (WB36) had a material cost of 1281×10^3 VND/m³. The BA30 mix showed a 5.79% increase in cost (to 1355×10^3 VND/m³), while higher BA contents resulted in a variable increase/decrease in cost. BA50 showed a 0.74% increase (to 1290×10^3 VND/m³), BA70 had a 4.31% reduction (to 1225×10^3 VND/m³), and BA100 showed an 11.08% reduction (to 1139×10^3 VND/m³).

• Future studies could focus on enhancing the pozzolanic reactivity of BA using chemical treatments or admixtures, improving its performance at higher replacement levels (i.e., 50% BA), and optimizing mix designs for both strength and sustainability. Furthermore, the long-term environmental impact should be evaluated to assess the potential risk regarding the chemical or pollutant leaching from concrete containing BA.

Although this study demonstrates clear sustainability benefits in terms of reduced CO_2-eq emissions, EC, and natural sand usage, environmental safety aspects related to potential heavy-metal leaching from BA were not investigated. Leaching tests (i.e., TCLP or equivalent standards) should be conducted in future studies to verify long-term environmental compliance before field-scale implementation. Also, durability assessment in this study was primarily based on WA, porosity, and UPV, which provide indirect indicators of pore structure and permeability. Other performance-based durability tests, such as drying shrinkage, carbonation resistance, or chloride permeability, should be performed in future studies to further verify the long-term service performance of BA-containing concrete, particularly under aggressive exposure conditions.

It should be noted that microstructural characterization in this study was limited to raw materials due to the unavailability of preserved hardened concrete specimens after mechanical testing. Consequently, SEM investigation of the interfacial transition zone (ITZ) between BA particles and cement paste could not be performed. Future studies should include SEM analysis of hardened concrete, with particular emphasis on ITZ morphology, micro-cracking, and bonding quality, to directly validate the microstructural mechanisms underlying the observed strength reduction at high BA replacement levels.

References

[1] J.E. Kim, J. Seo, K.-H. Yang, H.-K. Kim. (2023). Cost and CO2 emission of concrete incorporating pretreated coal bottom ash as fine aggregate: A case study. *Construction and Building Materials*, 408, 133706. https://doi.org/10.1016/j.conbuildmat.2023.133706

[2] H. Kurama, M. Kaya. (2008). Usage of coal combustion bottom ash in concrete mixture. *Construction and Building Materials*, 22(9), 1922-1928. https://doi.org/10.1016/j.conbuildmat.2007.07.008

[3] G.M. Cuenca-Moyano, M. Cabrera, M. López-Alonso, M.J. Martínez-Echevarría, F. Agrela, J. Rosales. (2023). Design of lightweight concrete with olive biomass bottom ash for use in buildings. *Journal of Building Engineering*, 69, 106289.https://doi.org/10.1016/j.jobe.2023.106289

[4] N. Nakararoj, T.N.H. Tran, P. Sukontasukkul, A. Attachaiyawuth, W. Tangchirapat, C.C. Ban, P. Rattanachu, C. Jaturapitakkul. (2022). Effects

of High-Volume bottom ash on Strength, Shrinkage, and creep of High-Strength recycled concrete aggregate. *Construction and Building Materials*, 356, 129233. https://doi.org/10.1016/j.conbuildmat.2022.129233

[5] P. Chindasiriphan, B. Meenyut, S. Orasutthikul, P. Jongvivatsakul, W. Tangchirapat. (2023). Influences of high-volume coal bottom ash as cement and fine aggregate replacements on strength and heat evolution of eco-friendly high-strength concrete. *Journal of Building Engineering*, 65, 105791. https://doi.org/10.1016/j.jobe.2022.105791

[6] M.W. Ashraf, Y. Tu, A. Khan, A.S. Siddiqui, S. Mubarak, M. Sufian, S. Ullah, C. Wang. (2025). Experimental and explainable machine learning based investigation of the coal bottom ash replacement in sustainable concrete production. *Journal of Building Engineering*, 104, 112367. https://doi.org/10.1016/j.jobe.2025.112367

[7] P. Kiruthiga, N. Dave, S. Shahabuddin, R. Guduru. (2025). Development of sustainable concrete with pulverized coal bottom ash for low cost and carbon emission. *Construction and Building Materials*, 462, 139949. https://doi.org/10.1016/j.conbuildmat.2025.139949

[8] J. Li, H. Zhang, Y. He, X. Wang, X. Cao, H. Yang, L. Chen, S. Xu, H. Wen, L. Gu. (2025). The synergistic role of sludge conditioner FeCl3/Rice husk on co-combustion with coal gangue: Thermaldynamic behavior, gases pollutants control and bottom ash stabilization. *Journal of the Energy Institute*, 118, 101920. https://doi.org/10.1016/j.joei.2024.101920

[9] Z. Zhao, R. Wang, J. Wu, Q. Yin, C. Wang. (2019). Bottom ash characteristics and pollutant emission during the co-combustion of pulverized coal with high mass-percentage sewage sludge. *Energy*, 171, 809-818. https://doi.org/10.1016/j.energy.2019.01.082

[10] C.G. Arenas, M. Marrero, C. Leiva, J. Solís-Guzmán, L.F.V. Arenas. (2011). High fire resistance in blocks containing coal combustion fly ashes and bottom ash. *Waste Management*, 31(8), 1783-1789. https://doi.org/10.1016/j.wasman.2011.03.017

[11] ASTM. (2012). ASTM C143-12. Standard Test Method for Slump of Hydraulic-Cement Concrete.

[12] ASTM. (2017). ASTM C138. Standard Test Method for Density (Unit Weight), Yield, and Air Content (Gravimetric) of Concrete.

[13] ASTM. (2021). ASTM C39. Standard Test Method for Compressive Strength of Cylindrical Concrete Specimens.

[14] ASTM. (2021). ASTM C642. Standard Test Method for Density, Absorption, and Voids in Hardened Concrete.

[15] ASTM. (2016). ASTM C597. Standard Test Method for Pulse Velocity Through Concrete.

[16] F. Celik, O. Akcuru. (2020). Rheological and workability effects of bottom ash usage as a mineral additive on the cement based permeation grouting method. *Construction and Building Materials*, 263, 120186. https://doi.org/10.1016/j.conbuildmat.2020.120186

[17] T.S. Nguyen, M.Q. Thai, L.S. Ho. (2021). Properties of fine-grained concrete containing fly ash and bottom ash. *Magazine of Civil Engineering*, 107(7), 10711-10711. https://doi.org/10.34910/MCE.107.11

[18] A. Wongsa, Y. Zaetang, V. Sata, P. Chindaprasirt. (2016). Properties of lightweight fly ash geopolymer concrete containing bottom ash as aggregates. *Construction and Building Materials*, 111, 637-643. https://doi.org/10.1016/j.conbuildmat.2016.02.135

[19] M. Singh, R. Siddique. (2016). Effect of coal bottom ash as partial replacement of sand on workability and strength properties of concrete. *Journal of Cleaner Production*, 112, 620-630. https://doi.org/10.1016/j.jclepro.2015.08.001

[20] A.M. Neville. (2011). Properties of Concrete, 5th Edition [Book]. Pearson.

[21] S.E.E. Khay, J. Neji, A. Loulizi. (2010). Shrinkage properties of compacted sand concrete used in pavements. *Construction and Building Materials*, 24(9), 1790-1795. https://doi.org/10.1016/j.conbuildmat.2010.02.008

[22] H.K. Kim, H.K. Lee. (2011). Use of power plant bottom ash as fine and coarse aggregates in high-strength concrete. *Construction and Building Materials*, 25(2), 1115-1122. https://doi.org/10.1016/j.conbuildmat.2010.06.065

[23] H. Hamada, A. Alattar, B. Tayeh, F. Yahaya, A. Adesina. (2022). Sustainable application of coal bottom ash as fine aggregates in concrete: A comprehensive review. *Case Studies in Construction Materials*, 16, e01109. https://doi.org/10.1016/j.cscm.2022.e01109

[24] R. Siddique. (2013). Compressive strength, water absorption, sorptivity, abrasion resistance and permeability of self-compacting concrete containing coal bottom ash. *Construction and Building Materials*, 47, 1444-1450.https://doi.org/10.1016/j.conbuildmat.2013.06.081

[25] M. Singh, R. Siddique. (2014). Strength properties and micro-structural properties of concrete containing coal bottom ash as partial replacement of fine aggregate. *Construction and Building Materials*, 50, 246-256. https://doi.org/10.1016/j.conbuildmat.2013.09.026

[26] M. Singh, R. Siddique. (2015). Properties of concrete containing high volumes of coal bottom ash as fine aggregate. *Journal of Cleaner Production*, 91, 269-278. https://doi.org/10.1016/j.jclepro.2014.12.026

[27] H.K. Kim, J.H. Jeon, H.K. Lee. (2012). Flow, water absorption, and mechanical characteristics of normal- and high-strength mortar incorporating fine bottom ash aggregates. *Construction and Building Materials*, 26(1), 249-256. https://doi.org/10.1016/j.conbuildmat.2011.06.019

[28] M. Rafieizonooz, J. Mirza, M.R. Salim, M.W. Hussin, E. Khankhaje. (2016). Investigation of coal bottom ash and fly ash in concrete as replacement for sand and cement. *Construction and Building Materials*, 116, 15-24.https://doi.org/10.1016/j.conbuildmat.2016.04.080